GMCL #1254515, VOL 639, ISS 1

Model of 1D charge carrier traps and polyconformism of silicon backbone segments in the polymer poly(di-n-hexylsilane)

A. F. Gumenyuk and O. A. Kerita

QUERY SHEET

This page lists questions we have about your paper. The numbers displayed at left can be found in the text of the paper for reference. In addition, please review your paper as a whole for correctness.

There are no Editor Queries for this paper.

TABLE OF CONTENTS LISTING

The table of contents for the journal will list your paper exactly as it appears below:

Model of 1D charge carrier traps and polyconformism of silicon backbone segments in the polymer poly(di-n-hexylsilane)
A. F. Gumenyuk and O. A. Kerita

MOLECULAR CRYSTALS AND LIQUID CRYSTALS
2016, VOL. 639, 1–16
http://dx.doi.org/10.1080/15421406.2016.1254515

Taylor & Francis
Taylor & Francis Group

Model of 1D charge carrier traps and polyconformism of silicon backbone segments in the polymer poly(di-n-hexylsilane)

A. F. Gumenyuk and O. A. Kerita

Institute of Physics National Academy of Sciences of Ukraine, 46 Nauky Ave., Kiev, Ukraine

ABSTRACT

Studied an energy spectrum of traps in poly(di-*n*-hexylsilane) by fractional thermoluminescence. The spectrum is discrete, while the frequency factor is dispersed. It was found that this energies form three oscillatory series. Energy of the oscillatory quantum for each series coincides with the energy corresponding symmetrical Raman mode of the polymer silicon backbone. It is found that each oscillator series corresponds to a specific conformation of the silicon backbone. Model of traps was developed which adequately explain all observed thermoluminescent features of the material.

KEYWORDS

Thermoluminescence; trap; polysilane; segment; conformation

PACS

78.66.Qn; 7866.Qn; 71,38,-K

1. Introduction

Poly(di-n-hexylsilane) (PDHS) is a silicon-organic polymer. Its molecule contains a linear chain of σ-conjugated silicon atoms and hexyl side groups: $[Si(C_6H_{13})_2]_n$. In earlier works [1, 2] has been investigated the energy spectrum of traps in the film of PDHS by fractional thermoluminescence (FTL). We have improved this method and mathematical processing of the experimental results, in particular, accounting a background-tunneling luminescence [1], which allowed significantly enhance an accuracy of determining the energy traps. It was established that energy traps in this material exhibit discontinuity whereas frequency factor is dispersed [1]. In the next paper [2] on the basis of additional experimental studies it was found that the energy traps in PDHS form two series that describes a generalized oscillator formula

$$E = n'\hbar\omega_\iota, \tag{1}$$

where $n' = 1$ for the initial energy of series, and takes half-integer values for following energies. The energy quantum $\hbar\omega_1 = 0.046$ eV and $\hbar\omega_2 = 0.033$ eV for series 1 and 2, respectively, coincides with the energies of individual Raman lines related to symmetric Raman modes of the silicon backbone.

In this paper we present results of a detailed study of traps energy for PDHS in low-temperature range (5–30 K). It was found another oscillatory series with energy quantum $\hbar\omega_3 = 0.0175$ eV (series 3) which also corresponds to the Raman line. In addition, the trap with energy of 0.012 eV was found which is expected to give rise to another series (series 4).

These results allowed us to develop a more advanced and compelling model of 1D-traps in PDHS the beginning of which are set out in [2]. In addition, it was to establish an existence

CONTACT A. F. Gumenyuk Gumenyuk_af@ukr.net

at least three conformations of the silicon backbone in our fabricated PDHS films: *anti trans, trans gauche* (TG_+TG_-), and *deviant* (7/3 *helix*). Series 4 relate presumable to the *transoid* (15/7 *helix*) conformation.

2. Experimental results

The reason that prompted us to conduct an additional studies of energy traps in PDHS, was a presence in some samples of the trap with energy 0.0175 eV which is not included in the above two oscillatory series [2]. We assume that this energy opens a new oscillatory series. For that purpose a detailed study of FTL in low-temperature range 5–30 K were carried out. To obtain a sufficient number of fractions in this narrow temperature range, a sensitivity of the intensity channel was increased by 24 times, compared to the previously used conditions [1, 2]. As a result, in this temperature range it was obtained ~100 fractions (conventionally sample 1). Calculated fractional energies plotted by dots in Fig. 1 depending on the effective temperature of fractions. The last was calculated for the maximum values of the fraction intensity which were everywhere the same. Energy traps are identified by accumulation of points indicating that the same trap is emptied. This way to present a data allows estimate the temperature range in which take place an intense liberation of the same type traps. Solid curve 2 shows the intensity of thermoluminescence (TL) from sample 1.

Figure 2 shows these energies as a function of sequence fraction numbers. In this case, data are arranged uniformly along the abscissa and traps energy identified by presence of shelves in a graph. As compared with previous way the trap energies were determined more reliably. For example, it was possible to identify trap with energy 0.048 eV, the presence of which in Fig. 1 is doubtful. Two energy 0.0323 and 0.0482 eV relates to a series 2, ($n' = 1$ and 1.5, respectively). Three remaining values: 0.0176 ± 0.0002, 0.0267 ± 0.0001, and 0.0433 ± 0.0002 eV form, as expected, a new series 3 ($n' = 1$, 1.5, and 2.5, respectively). In addition, a new trap with energy $E = 0.012$ eV was found. Stars denote a result of re-control study. We assume that this trap open a new oscillatory series (series 4) which is built on the same principle as previous series. Unfortunately, the identification of other traps energy of this series is not possible because the next energies 0.018 ($n' = 1.5$), and 0.030 ($n' = 2.5$) eV actually coincides with initial energies of series 3 and 2 (0.0175 and 0.032 eV, respectively).

Fractional studies of the sample 2 were carried out under the same conditions as for a previous sample except that experiments were continued to complete emptying of all traps.

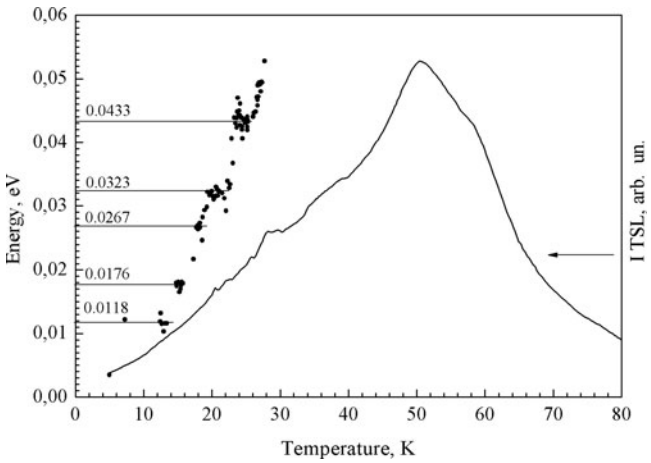

Figure 1. TL of PDHS, sample 1. Glow curve (line); fraction energies versus the effective temperature (circles).

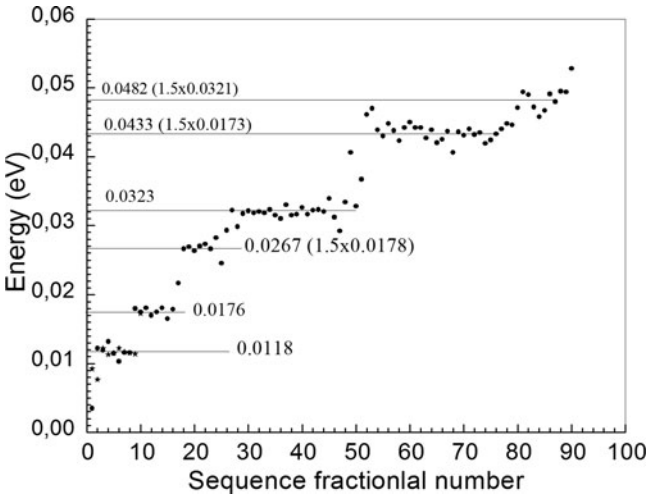

Figure 2. Energy dependence versus the fractions sequence number, sample 1.

Figure 3 shows the energies versus the sequence number of fractions. All energies belong to series 3 ($\hbar\omega_3 = 0.0175$ eV): 0.0260 ± 0.0002, 0.0442 ± 0.0004, 0.0622 ± 0.0004, and 0.0781 ± 0.0005 eV. In this sample, the trap with the initial energy 0.0175 eV not detected, but found two new traps: 0.062 and 0.078 eV.

Energies found in [1, 2], as well as found in a present study [1, 2] are shown in Fig. 4 in the form of four oscillatory series (series 4 hypothetical). Here *n*' means the ratio of the trap energy to the vibration quantum energy $\hbar\omega_i$ of *i*th series. The charge liberation take place by means of a thermal process, therefore the energy quantum $\hbar\omega_i$ which generates an oscillatory series should be mapped to the vibration spectra of substance. Indeed, in the Raman spectrum of PDHS among others there are lines 373 cm^{-1} (0.0463 eV), 259 cm^{-1} (0.0321 eV), and 147 cm^{-1} (0.018 eV) (Fig. 5) what practically coincide with $\hbar\omega_{1,2,3}$, respectively. The Raman line of 97 cm^{-1} (0.012 eV) which would be responsible for formation of series 4, we have not detected. In the relevant literature all data are presented starting with the values not less than 100 cm^{-1}. Unbiasedness of lines in low-frequencies Raman spectrum (100–500 cm^{-1})

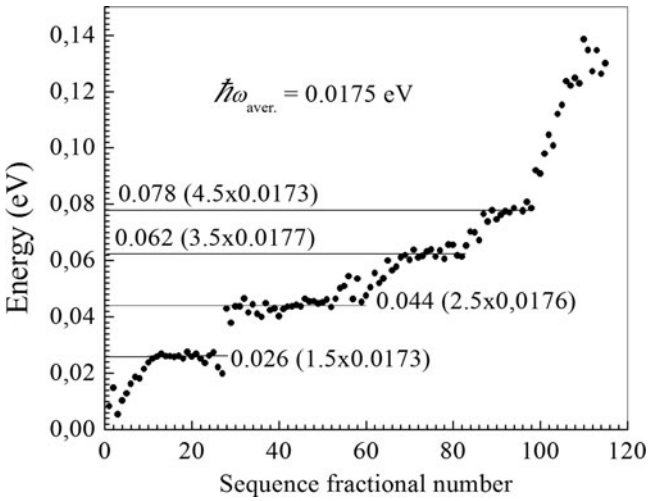

Figure 3. Energy dependence versus the fractions sequence number, sample 2.

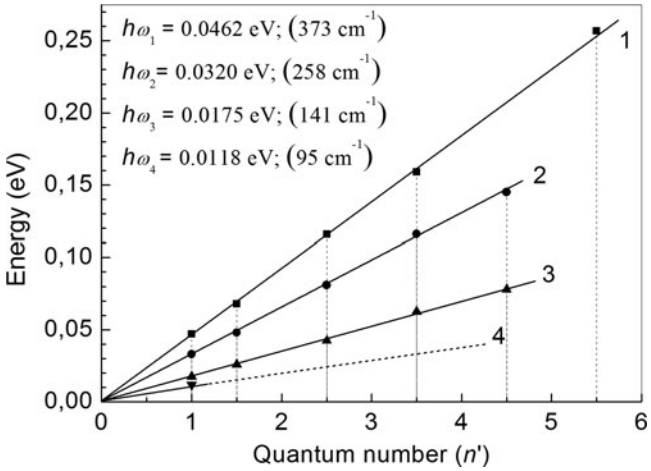

Figure 4. Oscillator series of energy traps in PDHS.

for a ^{13}C enriched samples indicates that these lines are due to vibrations of the silicon backbone [3]. Study of oriented PDHS samples allowed authors of this paper conclude that the line 373 cm^{-1} belongs to the symmetric Raman mode of silicon backbone of the all-trans conformation.

3. Discussion

3.1. Developing of traps model in PDHS

In this section, a model of traps, that should explain a next non-trivial TL features in the studied polymer, is offered: (i) Existence of traps with discrete energies and simultaneously dispersible character of frequency factor [1, 2]. (ii) Presence of a few oscillatory series in an

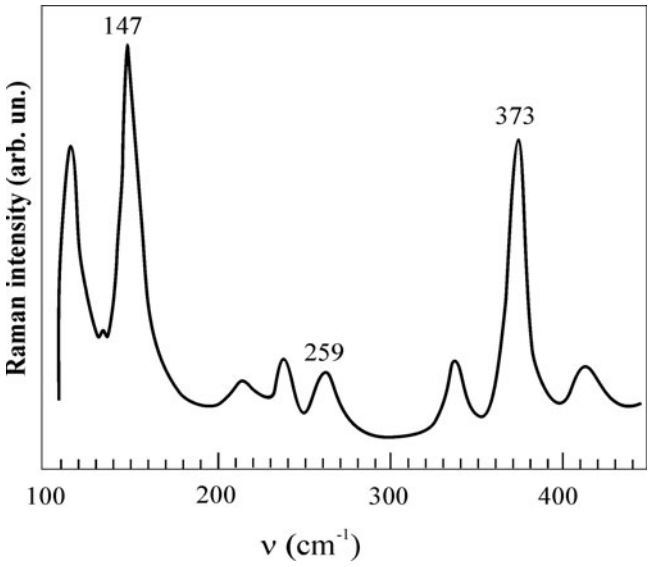

Figure 5. Raman spectrum of PDHS powder at room temperature.

energy spectrum of traps. (iii) A correlation between the traps energy and separate frequencies in Raman spectrum of PDHS. (iv) It is necessary to explain why the first energy in each series coincides with energy of the corresponding vibration quantum in the Raman spectrum, whereas next energies answer to a half-integer value of this quantum.

In addition to our experimental data, we leaned against such reliably fixed facts: (1) Traps for holes are segments of polymeric chain of the different lengths. Within the segment, there is regularity in the mutual orientation of the Si–Si bonds, i.e., there is a translational symmetry of silicon backbone [3–5]. The segments are separated by conformational defects caused by violations of the regularity of silicon backbone that, in turn, violates translational symmetry of the silicon backbone [4–7]. Furthermore, a branch point may be a boundary of the segment [8]. The hole created by UV irradiation at liquid-helium temperatures is delocalized within the segment when intersegment defects form barriers to moving of the holes along silicon backbone [4, 9, 10].

b) A captured hole polarizes a neighboring environment, i.e., forms the polaron [11–13].

The well depth with captured holes is determined by a few factors. First of all, it is necessary to take into account that as traps in linear polymers are the segments of the silicon backbone, whereas in conventional 3D crystals this function is performed by point defects. Consequently, appear a new parameter – length of the segment, which affects depth of a potential well. Indeed, since there is a trend to polymerization, then lower electron energy correspond a longer chain. Quantitative estimates of this dependence on the basis of uncertainty relation can be written as

$$\Delta pL \geq \hbar \tag{2}$$

where L denotes the length of segment and Δp is a momentum uncertainty. Taking into account one-dimensional motion, get, that an uncertainty for kinetic energy ΔE is

$$\Delta E = \frac{\hbar^2}{2Ma^2n^2}, \tag{3}$$

where $L = na$, a is a distance between adjacent Si atoms, and n is an amount of Si–Si bonds in segment. A formula (3) describes a quantum-size effect which plays an important role in a nanophysics. Equation (3) shows that an additional kinetic energy is essential for a short segment and falls rapidly to the zero if L increases.

Another factor influencing on the well depth, is a type of a conformational defect, which determined by the rotation around of the Si–Si bond at angles that differ from a regular sequence them into a segment. Calculations specify on existence in polysilanes a few values of these turning (dihedral or torsion) angles [6, 7].

Another factor significantly affects the depth of potential well, is a presence of the excited electron on the boundary of the segment in that there is a hole, because its Coulomb potential significantly reduces the height of barrier for holes. Also need to take into account the energy of relaxation of the polarized environment.

The presence of a few factors differently influence on the depth of well, eliminates existence of any simple distribution pattern of these depths. Moreover, the mechanism related to variable segments length, determines an asymptotic reduction of discreteness in distribution of these depths with the increases of length of the segment (Eq. 3). At the same time an experimental distribution of trap energies exhibit discreteness comparable with the values of energies themselves. Accounting of these factors leads to the conclusion that *the energy discreteness should be characterize each potential well*. In fact, this conclusion is derived from

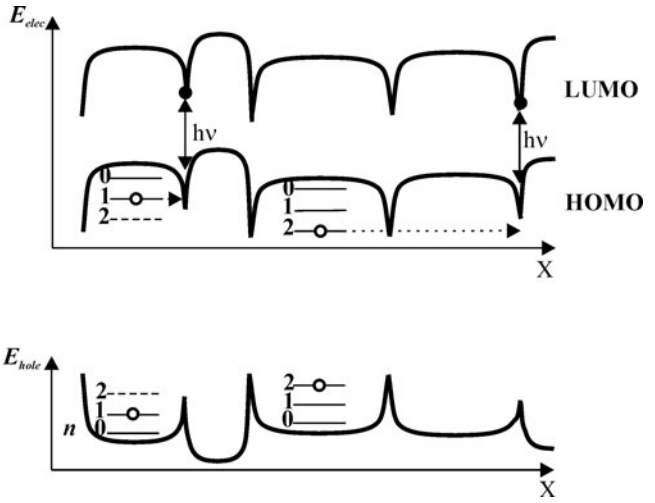

Figure 6. Scheme of electronic structure of PDHS.

quantum mechanical postulate about the finite nature of the particles motion. Thus, *distribution of energy levels is determined by a feature of the interaction excess charge with the nearest surrounding*. An observed regularity in the energy spectrum of traps indicates an elastic nature of forces acting on the hole, i.e., determines the interaction due to the polarization. Thus, excess holes forms polarons in PDHS.

The presence of the discrete states in the well means, that ~~has~~ depth does not determine of the energy of traps; it limits the amount of bound oscillatory states only. Liberation of the holes occurs from an excited vibration levels by tunneling through the potential barrier created by a conformational defect.

A further analysis is conveniently carried out using Fig. 6, which shows the band diagram f[illegible]he straightened silicon backbone. At the bottom shows schematically the holes energy $U_{hole} = e\varphi$. Each well corresponds to a separate silicon backbone segment. It is important to notice that existence of barrier for the hole means existence of some effective positive charge that, probab[illegible]ises up as a result of the bend of polymeric chain in the boundary of segment. We can get an energy profile of electron (as the opposite charge) by mirror reflecting of the holes profile($E_{elec} = -e\varphi$). Middle curve represent the profile of top of valence band, the upper curve, accordingly, profile of bottom of conduction band. The dependence of well depth on length of segment qualitatively accounted in the diagram. Also a significant decrease of the barrier height is taken into account to the presence of excited electron on the boundary. Note that the vibration levels are shown conditionally for the sake of clarity, since the X-axis describes the straightened distance along a chain, while configuration coordinate determine the energy of oscillator and, essentially, is a differential which describes atom displacements with respect to the lattice site.

Character of potential profile for electronic energy allows to assume that excited electron must be localized on the segment boundary. Indeed, if an end of segment to be a barrier for the hole, then for an electron there is a well in this place. The diagram shows, that excited electron is placed in narrow potential well which separates from the other well a wide barrier (strong localization), whereas a hole in the valence band, on the contrary, be in a wide valley separated from a next valley by narrow barrier (delocalization in the segment). Therefore the tunneling probability of the holes through a narrow barrier is significantly higher, than electrons. Indeed, in this polymer there is a holes photoconductivity that testifies to the considerable degree of

localization of non-equilibrium electrons in compared to the holes [4, 9, 11, 14, 15]. Thus, the model includes mechanisms of localization of excited carriers of both signs that is an obligatory condition for existence of TL.

TL process includes a large number of particles. Therefore correct approach to the problem is a thermodynamic approach, rather than consideration of behaviour of separates particle. For this purpose will consider thermal processes in an ensemble of m quantum oscillators that represent a system of m polaronic traps with identical energy of thermal activation. A phonons absorption and emission kinetic is described by the $N + 1$ balance equations:

$$\begin{aligned}
\frac{dm_0}{dt} &= f_{1,0}m_1 - f_{0,1}m_0 \\
&\vdots \\
\frac{dm_i}{dt} &= f_{i-1,i}m_{i-1} - f_{i,i-1}m_i - f_{i,i+1}m_i + f_{i+1,i}m_{i+1} \\
\frac{dm_{i+1}}{dt} &= f_{i,i+1}m_i - f_{i+1,i}m_{i+1} - f_{i+1,i+2}m_{i+2} + f_{i+2,i+1}m_{i+2} \\
&\vdots \\
\frac{dm_N}{dt} &= f_{N-1,N}m_{N-1} - f_{N,N-1}m_N - fm_N
\end{aligned} \tag{4}$$

Here m_i means the amount of the states with energy $E_i = \hbar\omega(i + 1/2)$; $f_{i,i+1}$ describes transition rate $i \to i + 1$, i.e., disappearance of one center with energy E_i due to the phonon absorption, and simultaneously increment the amount of centers with energy E_{i+1}. On the contrary, the emission of phonon by the center with energy E_i decrements amount of this type centers and, accordingly, increments amount of the centers with energy E_{i-1}. The last equation describes liberation of charge from the last, N^{th} oscillator bound state by its tunneling. Adding all equations (4) with $f_{i,i+1} = f_{i+1,i}$ we obtain

$$\frac{dm}{dt} = -fm_N \tag{5}$$

TL is a quasi-equilibrium process, as the rate of change of temperature is much lower, than the rate of microscopic processes, i.e., the rate of phonons exchange between a center and thermostat that is an environment. Therefore probability of existence of trap in Nth quantum state is determined by a Boltzmann's function

$$w_N = \frac{m_N}{m} = \frac{1}{A}\exp\left(-\frac{E_N}{kT}\right), \tag{6}$$

where A is a statistical factor. Substituting this expression in (5), we have

$$\frac{dm}{dt} = -s_0 m \exp\left(-\frac{E_N}{kT}\right), \tag{7}$$

This equation describes linear kinetics of TL, where the proportionality factor $s_0 = f/A$ called as frequency factor. During heating, the population of excited states increases according to the Boltzmann distribution. Equipment detects a desired signal, as soon as the amount of charges overcoming barriers per unit time exceeds of the threshold equipment.

3.2. About a disperse character of the frequency factor

In conventional 3D crystal, a nearest environment for of the same type traps to be identical, thus, identical will be transparency of potential barriers. Therefore a frequency factor s_0 for these traps must be unchanging. For the segment model of traps, transparency of barrier is a variable depending on the mechanisms influencing on the depth of the well. For the barrier of arbitrary shape its transparency described by formula

$$D = D_0 \exp\left[-\frac{2}{\hbar}\int_{x_1}^{x_2}\sqrt{2M\,(U - E(x))}dx\right]. \tag{8}$$

Here E is energy of particles, M – of its mass, U is the height of barrier, $x_2 - x_1$ it's width of barrier at the energy level. The expression $mexp(-E/kT)$ in (7) has a global meaning, as describes the amount of particles having the energy E. Therefore the parameters of concrete substance must be included in s. That is

$$s_0 = s_1 D = s_1 D_0 \exp\left[-\frac{2}{\hbar}\int_{x_1}^{x_2}\sqrt{2M\,(U - E)}dx\right], \tag{9}$$

where, in this case $E = \hbar\omega(n + 1/2)$ and s_1 is a new proportionality factor.

The height of barrier varies randomly according on combination of the mechanisms described above. A maximal transparency of barrier answers a case, when his coincides with the Nth level ($U = E_N$), i.e., a maximal value of frequency factor is $s_{max} = s_0 D_0$. Thus always $D_0 < 1$, as particle can be reflected from barrier even in the case when its energy exceeds his height. Minimum transparency of barrier answers the case, when his almost reaches the next level ($U - E_N \leq \hbar\omega$). Thus, dispersed nature of the frequency factor follows naturally from this model.

Value of frequency factor for the elementary glow curve (7) can be calculated by examining this function on a maximum that gives

$$s = \frac{E\beta}{kT_m^2}\exp\left(\frac{E}{kT_m}\right), \tag{10}$$

$\beta = dT/dt = const$ – heating rate, T_m – temperature of the maximum glow curve (7).

As proof of dispersible character of the frequency factor on Fig. 7 one of the results driven to work [2] is recreated. Curve 1 represents the glow curve from PDHS film; 2 depict the energies of fraction depending on an effective temperature. Shelves on this dependence testify to existence of traps with discrete energies. However TL curve lacks any reliable features that can be attributed to the concrete traps. At the same time, glow curves 3, 4 calculated according to (7) for energies helves with T_m correspond to the high-temperature ends of shelves, almost not overlap. Existence of discrete energies of traps and simultaneously lack of appropriate distinct peaks on the glow curve is possible only, if to assume dispersible character of frequency factor.

Consequently, in the temperature range, where traps with the same energy emptied, the frequency factor (Eg. 9) diminishes from fraction to fraction (according to various shelves on 4–7 orders of magnitude). It means that in the temperature range corresponding to the width of shelf, TL intensity is a superposition of elementary curves (Eq. 7) with identical energies and frequency factor, which falls with the increase of temperature that result in blurring of resultant glow curve. It should be noted that in some samples, the glow curve exhibit weak recreated features that correlates with placing of shelves, as it can be seen on Fig. 1. Absence of distinct TL peaks, that would answer concrete trap, is not an obstacle for the fractional method since each fraction is a superposition of exponential curves with different intensities I_{0i}, but

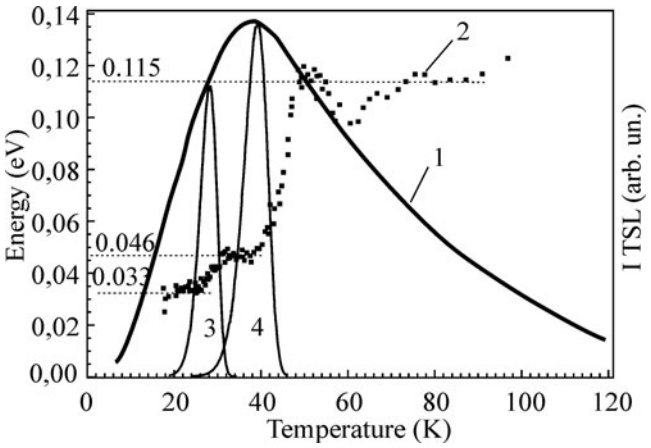

Figure 7. TL of PDHS film. 1 - glow curve; 2 - energies of fraction depending on an effective temperature; 3, 4 - glow curves calculated for the energies 0.033, 0.046 eV and $T_m = 28$, 40 K corresponding to the ends of shelves, respectively [2].

with the same exponent:

$$I = \sum \delta I_{0i} \exp\left(-E/kT\right) = I_0 \exp\left(-E/kT\right), \tag{11}$$

where $\delta I_{0i} = \delta m_i s_i \approx const$ integrates trap with the same s_i.

In principle, the holes can tunnel from all oscillator states, but with different probabilities. For shallow traps ($n' = 1, 1.5$) it is important to consider also transitions from the ground level ($n' = 0$) as a result of considerable concentration of the filled traps in this state, that equals the concentration of all filled traps practically, and also as a result of enough considerable transparency of barrier to this level. During cyclic emptying of low-temperature (5–45 K) traps from the level $n = 0$, their concentration drops from fraction to fraction (as it can be seen on Fig. 2), i.e., for the traps of all series with $n' = 1, 1.5$. Therefore to obtain of correct values of energies, intensity of this background was subtracted from intensity of corresponding fractions suggesting it unchanged within the fraction (more detail in Ref. 1).

3.3. Conformity TL and raman frequencies

A next problem was to find out the reasons of correlation between energies $\hbar\omega_{1,2,3}$ generating oscillatory sequences and Raman modes of the silicon backbone. The polarization distortion, created by a point charge, has central symmetry so to release the charge carrier, the nearest environment must interact with vibration mode of the same symmetry, i.e., with A_g mode. Indeed, polarization distortion is a static displacement of neighboring charges towards the excess charge or from it, depending on the charge sign. In the case of symmetric vibration mode the charges environment oscillate along the same directions. With increasing amplitude due to the absorption the required amount of phonons, oscillating ions environment in some moment of time take the position close to those in an unperturbed lattice, i.e., polarization distortion disappears practically. In next moments of time, up to the points of turn, a potential hill grows in this place. Sliding down from this hill, the charge will have an additional opportunity to leave the trap. Thus, energy quantum that generate of oscillatory series should coincide with the energies of the symmetric Raman modes. As marked higher, frequencies of

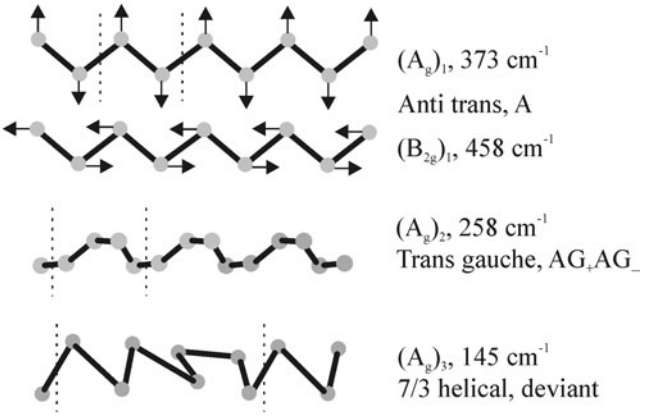

Figure 8. Examples of the silicon backbone conformations; dashed lines separates the unit cells.

separate Raman lines coincide with TL frequencies generate series of 1, 2, 3. Corresponding Raman frequency for the series 4 not yet detected.

Will mark that displacement of ions in the central field of charge falls with distance from it, while amplitude of A_g-oscillation everywhere is identical, therefore ideal compensation of distortion is impossible. In this connection even during the most favorable configuration of ions there will be some potential barrier, what charge must overcome.

Oscillatory law in the energy spectrum of PDHS is not unique to just this material. This law has been established earlier in many inorganic ion-covalent crystals. Among them are known crystals of oxides [16 a-d], alkali halides [16 e-g], and other. Depending on the complexity of lattice structure it was observed from one in Al_2O_3 [16 d], to five in $Y_3Al_5O_{12}$ [16 a] oscillatory series. In crystals with the structure that allows the existence of Raman-active modes, there always is a Raman line whose frequency coincides with the frequency generated the corresponding oscillatory series. The simple cubic lattice of the alkali halides does not allow the existence of the Raman active modes. However, they also exhibit an oscillatory law in the energy of traps (singly-serial everywhere). The energy of TL quanta in alkali halides coincides with activation energy of mobility of H-centers for the given crystal [16 f, g].

3.4. Polyconformism of PDHS films

It was assumed in earlier studies [3, 4, 6], that PDHS in solids at temperatures below the order-disorder transition($< 42^oC$), is a highly ordered polymer with all-trans conformation of the silicon backbone (anti-trans, A-trans or just A, according to Ref. 7). Torsion angle for this conformation, $\tau = 180°$, so the silicon backbone is a planar zigzag chain (Fig. 8). Unit cell contains two Si atoms and belong to D_{2h} point group, i.e., there are two Raman-active modes: 373 cm^{-1} (0.0463 eV) and 458 cm^{-1} (0.0568 eV) with symmetry A_g and B_{2g}, respectively [3]. Thus, series 1 ($\hbar\omega = 0.046$eV) is generated by A-trans conformation of Si backbone. Atomic displacements corresponding to these vibration modes can be seen on Fig. 8.

It is known that low-frequency region $100 < \nu < 500$ cm^{-1} in the Raman spectrum presented solely by vibration modes of silicon backbone as evidenced by immutability of their position in ^{13}C enriched samples [3]. An amount of Raman lines in this area (three triplets in Fig. 5) exceeds the value predicted for A-trans conformation, so it is naturally to assume that molecules in the solid polymer contain of backbone segments with alternating conformations

and each of them have their own frequency due to the internal vibrations in the unit cell, i.e., relates to optical modes. This is also evidenced by the presence of several oscillatory TL series because each of them should correspond to own symmetric vibration mode.

Series 2 generated by TL quantum with energy 0.032 eV and answered by Raman frequency of 259 cm^{-1} (Fig. 5). According to above assumption, it must be a symmetric vibration mode of the backbone another conformation (not A-trans). In search of a suitable conformation, we noticed that the frequency ratio of series 1 and 2 is $\sqrt{2}$ $[(\hbar\omega_1/\hbar\omega_2)^2 = 2.07 \approx 2]$. As noted in [17], the SiSiSi angle between adjacent bonds does not depend on the type of conformation, therefore, in a first approximation, the dynamic coefficient should not depend on it. So the resulting ratio corresponds to the oscillation mass equal to the mass of two Si atoms. This condition corresponds to the *trans-gauche* conformation (TG_+TG_-), that, as well as all next conformations, already is not planar (Fig. 8). Indexes + and – refer to the right and left torsion angle, that approximately equals the half of value of angle between the Si–Si bonds, $\tau \sim 55°$ [18–20]. From Fig. 8 evidently, that unit cell of this ladder structure contains four Si atoms, and the optical (internal) oscillations occur between the halves of unit cell, each of that contains two silicon atoms.

For series 3 haves $\hbar\omega_3 = 0.0175$ eV ($141 cm^{-1}$). This frequency corresponds to the Raman line of 147 cm^{-1} (0.18 eV), Fig. 5. We could not found the published data on the symmetry of this mode, and our measurements performed on non-oriented samples. However, based on the coincidence of Raman and TL frequencies in the two previous cases as well as the results of previous works [16 a–d] it can be assumed that this mode is also full-symmetric. Based on the magnitude of the relationship: $(0.0462/0.0175)^2 = 6.97 \approx 7$, this vibration mode must correspond to the joint oscillation of heavy clusters consisting of seven silicon atoms. Conformation which corresponds to this condition, known as 7/3 *helix* [4, 18, 20] or *deviant*, D_+, D_- [7] (Fig. 8). The Si–Si bonds form a polygonal helix around molecular axis. The unit cell contains seven silicon atoms. Within the unit cell Si–Si bonds make three full turns, so the torsion angle $\tau = 360 \times 3/7 = \pm 154^o$.

Finally, for the singly member of the series 4 appropriate expression $(0.0462/0.0118)^2 = 15.3 \approx 15$, i.e., cluster contains 15 silicon atoms oscillating in phase. Conformation with the unit cell consisting 15 atoms of silicon, known as 15/7 *helix* (transoid, T [7]). 15 Si–Si bonds perform seven complete turns within the unit cell, i.e., $\tau = \pm 168^o$. Existence of this conformation results from quantum-chemical calculations and finds experimental support, for example, from the X-ray diffraction data [21–24].

Note that the presence of multiple conformations in the same molecular chain means that conformational defect may not only be a single violation of the chain regularity, but the boundary between the silicon backbone segments with different conformations.

Accordance between Raman frequencies of the silicon backbone and types of it conformation is confirmed by data for poly(di-*n*-methylsilane) (PDMS) [25]. Here, in the 100–500 cm^{-1} region observed four Raman lines: 140, 188, 268, and 373 cm^{-1}, the latter two of which assigned to symmetric modes. Three frequencies almost coincide with frequencies creating series 1, 2, 3 in PDHS. For frequency of 188 cm^{-1} (absent in PDHS) ratio $(373/188)^2 = 4$, i.e., determines the oscillation frequency of cluster consisting of four silicon atoms. The conformation corresponding to this condition is known as O, ortho [7], $\tau = \pm 90^o$ (previously 4/1 helix). Thus in the PDMS sample used to the Raman study in [25], coexist four conformations: T, D, O, and A in the order according to the above frequencies list.

Theoretical calculations of the intramolecular potential energy $U(\tau)$ of the isolated molecules of oligosilanes with different hydrogen substituents found [18, 20, 26] the several, similar in depth, minima for the torsion angle τ referred to above for corresponding

conformations. It was found that increasing the molecules length or the side chain lengths as well as stay the polymer in solution or in solid state do not create new conformations, but only changes in different ways the wells depth, forming a preference for one or another conformation [20, 27, 28]. For example, isolated or dissolved PDHS molecules have basic conformation of 7/3 helix, whereas in solids dominate A trans conformation [26].

At temperatures above the phase transition (42 K), the side chains are melted which causing partially disordering of the silicon backbone. Due to intense thermal motion, in separate parts of the backbone appear and disappear the random conformations, i.e., "populated" and "depopulated" corresponding states of $U(\tau)$. Subsequent rapid cooling freezes this high-temperature polymorphic structure, which then slowly relaxes into a state typical for the low temperature. Really, it is found [30, 31], that after heating of PDHS films to 100–125 °C and subsequent quenching to 20°C and holding at certain intermediate temperatures, instead a broad absorption band $\lambda_{max} = 375$ nm attributed to $\sigma - \sigma*$ transitions, appear three narrower bands of 358, 374, and 385 nm. Structural complication of UV absorption spectra was observed also in polymer solutions after quenching it to temperature below 0°C [31]. Such transformation of UV spectra after similar temperature treatments was also observed in symmetrically and asymmetrically substituted polysilanes with other alkyl side chains [32, 33]. In all cases, these transformations are explained by the polymorphic structure of the silicon backbone. We also performed heat treatments of PDHS films before of TL study. After treating, the shape of glow curve can substantially change, and this property was used for the receipt as possible of more complete spectrum of traps.

Detection of polyconformism in the fluorescence spectra of PDHS is complicated by the fact, that exciton before its annihilation migrate from their birth place in the place with lower energy, i.e., in segment of greater length and/or in the segment with low-energy conformation. Therefore, to observe the fluorescence spectra from each individual conformation it is necessary to eliminate the migration of exciton along polymorphic chain, for example, to introduce linear molecules into the porous substrate. Indeed, any conformational defect distorts the molecular axis so the straight pore with the small diameter can be introduced the molecule (or part of it) as a single segment of certain conformation. Fluorescence studies [34, 35] to the composite consisting of porous silicate SBA-15 (pore diameter 10 nm) and PDHS molecules embedded in these pores showed that instead of a broad structureless band with a maximum at 365 nm in PDHS films, a new structure arises consisting of three narrower bands with maxima at 337, 355 and 369 nm. The splitting of the exciton band fluorescence indicates that the polymer molecules are introduced into the pores as single segments of three different conformations.

3.5. Traps energy spectrum of composite MCM-41:PDHS

Based on the ability of the porous material to separate individual conformations, energy spectrum of traps in the composites should be simplified compared to films. In order to test this hypothesis we undertook a study of the energy of traps in the composite MSM-41:PDHS. The molecules of polymer were introduced in the pores having a diameter of 2.8 nm from a solution in toluene. Results are shown in Fig. 9. 1 represents glow curve of composite. For comparison curve 3 shows glow curve from the film. Evidently, that the glow curve width of composite is much narrower than that for film. At the same time, it is much broader than those for elementary glow curve calculated according to (7) for $E = 0.032$ eV (curve 4). Squares depict the fractional energy most of them are placed on a single shelf with energy of 0.031 eV.

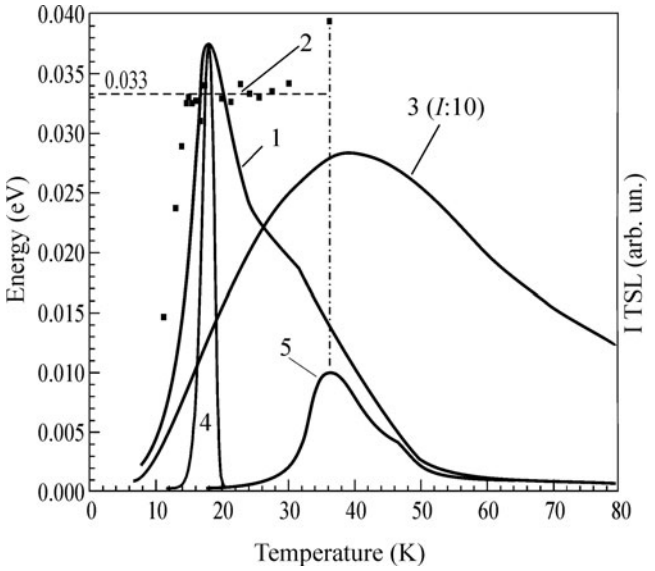

Figure 9. TL features of composite MSM41:PDHS. Glow curve (1); fractional energies (2); glow curve from film (3); calculate glow curve for $E = 0.32$ eV (4); last fraction (5).

This energy is a generator of series 2 and indicate occurrence of trans-gauche conformation. Relatively large half-width of the curve 1 and, at the same time, the presence of mono-energetic traps indicates a dispersed nature of the frequency factor also for the composite, which is probably due to the different lengths of the conformers.

Curve 5 represents of $I(T)$ for the last fraction. The value of energy determined from the initial rise ($\sim$ 0.04 eV) is underestimated because it does not criterion of constancy of m. However, as is clear from (7), the plot $\ln(I/m)$ versus $1/T$ is rectilinear in the entire temperature range. Thus obtained value of 0.047 eV practically coincides with the energy quantum generating of the series 1. This indicates the entry into pores also A trans conformers. A content of A trans conformation estimated from the areas under fractions does not exceed 20% of that for the trans gauche conformation. Thus in pores with diameter of 2.8 nm are located mainly trans-gauche conformers (series 2) and in small amount A trans (series 1), wherein this series are presented only by its initial energies.

3.6. Integer and half-integer values of energies

Does another problem that is decided on the basis of the worked out model of traps touch to finding out of question, why does energy of the first trap of every series coincide with the energy of corresponding Raman mode, while next energies answer the half-integer value of energy of this mode? First of all, we note that the universality of this pattern suggests a common mechanism of formation of oscillatory series for all conformations found in PDHS. We consider that this feature due to the difference of recombination mechanisms of liberated holes with localized electrons. If excited electron is located on the segments edge in which there is a hole, then recombination occurs directly from excited vibration state of the hole without moving it to neighboring segment. If such electron absent, then hole must tunnel through one or several barriers before recombination occurs. The difference between these two mechanisms manifested in particular normalization probability a thermal release of charge. In general, this

probability is given by

$$w_N = \frac{g_N \exp\left[-\frac{E_N}{kT}\right]}{A} \tag{12}$$

where E_N is energy of the level from which the charge is released; A is a statistical sum found from the normalization condition; g_N is a statistical weight of the state. For one-dimensional oscillator $g_N = 1$ and $E_N = \hbar\omega(N + 1/2)$. Summing (12) over all bound states we get

$$A_{osc} = \exp\left(-\hbar\omega/2kT\right) \frac{1 - \exp\left[-\hbar\omega\left(N+1\right)/kT\right]}{1 - \exp\left[-\hbar\omega/kT\right]}. \tag{13}$$

Since $\exp(-\hbar\omega/kT) \ll 1$, then $A_{osc} = \exp(-\hbar\omega/2kT)$ and we obtain from (13)

$$w_N = \exp\left[-\frac{N\hbar\omega}{kT}\right] \tag{14}$$

Thus, if recombination of thermally excited hole with an electron takes place directly from its vibration state, i.e., without tunneling in a nearby segment, then energy is equal to an integer number of the vibration quantum. We have not observed energies with multipleness that exceeds unit, probably, due to significant reduction of the barrier height in the Coulomb field of excess electron.

In other cases, the excess electron is separated from the hole one or more segments, so the hole must tunnel through one or more barriers. Liberated hole has considerable potential energy equivalent to the Nth oscillator's level. Reflected from the back side of the barrier, hole acquire considerable speed, so the inertial polarization of ions component can be neglected (adiabatic approximation). Therefore, the motion of hot hole along the segment until the scattering event can be considered as the movement of the Bloch particle in the valence band of one-dimensional crystal. With this in mind, the statistical sum A must be supplemented by the band component A_{band}: $A = A_{osc} + A_{band}$. Due to the large statistical weight, the band component should significantly exceed the oscillatory component therefore $A \approx A_{band}$. In this case, we obtain an expression for the releasing probability in the form:

$$w_N = \frac{1}{A_{band}} \exp\left[-\frac{\hbar\omega\left(N+1/2\right)}{kT}\right], \tag{15}$$

i.e., the energy traps for remote electron-hole pair is equal to half-integer value of $\hbar\omega$.

Thus, all oscillatory series obey the same laws: the lowest energy (generator of the series) coincides with the phonon energy of A_g vibration mode of silicon backbone of the corresponding configuration, whereas the following energies equal to half-integer number of the vibration energy quantum. This conclusion confirms the results obtained for the composite. Indeed, the polymer chain may be introduced into the rectilinear pore as a single segment in which is "smeared" the excited hole. The electron is localized on the end of the segment facing the excitation. In this case, the thermal activation energy is equal to the energy of the vibration quantum of the corresponding conformation.

4. Conclusion

Thus, proposed model of the hole traps allowed to adequately explain all thermoluminescent features of PDHS films and composites with his participation. The existence of oscillatory dependence and correlation between the TL energies and energies of the symmetrical vibration modes previously been firmly established for the number of inorganic crystals. These

features are explained in the framework of the polaron model traps. However, the existence of discrete energy spectrum and simultaneously the disperse frequency factor was first discovered in PDHS. It was found that an unusual combination of these properties is due to the fact that the traps for holes in PDHS are segments of the polymer chain, rather than point defects, as in the conventional 3D crystals. In addition, each of these segments has a certain conformation and uncertain length.

The existence of oscillatory patterns in traps energy due to the high degree of ordering PDHS films (~80% [3]) that determines the existence of rather long segments (an average about 20 silicon atoms [4]). As a result, PDHS molecule can be represented as a sequence of chains of certain conformations, and one can speak about the existence of lattice optical modes characteristic of a given conformation.

The hypothesis regarding the localization of excited electrons on the segment boundaries requires quantitative confirmation of the quantum-mechanical calculation. It does not contradict the fact that the conductivity in this material has a hole nature. On the basis of this assumption is naturally explained by the existence of traps with energies that are equal to an integer and half-integer values of the vibration quanta. Equally important is a fact that it is not necessary to assume the existence in the molecule of the chemical defects – electron acceptors.

Acknowledgment

The authors thank Dr. N. Ostapenko for discussion and critical comments that have greatly improved the content of the work.

References

[1] Gumenyuk, A., Ostapenko, N., Ostapenko, Yu., Kerita, O., & Suto, S. (2012). *Chem. Phys.*, *394*, 36.
[2] Gumenjuk, A., Ostapenko, N., Ostapenko, Yu., Kerita, O., Suto, S., & Watanabe, A. (2012). *Low Temp. Phys.*, *38*, 932.
[3] Kuzmany, H., Rabolt, J.F., Farmer, B.L., & Miller, R.D. (1986). *J. Chem. Phys.*, *85*, 7413.
[4] Pope, M., & Swedberg, C.E. *Electronic Processes in Organic Crystals and Polymers* (Second Edition, Oxford University Press 1999).
[5] Michl, J. (1992). *Synthetic Metals*, 49-50, 367.
[6] Bukalov, S. S., Leites, L. A., Magdanurov, G. I., & West, R. (2003). *J. Orgmet. Chem.*, *685*, 51.
[7] Michl, J., & West, R. (2000). *Account of Chemical Research*, *33*, 821.
[8] van Walree, C. A., Cleij, T. J., Jenneskens, L. W., Vlietstra, E. J., van der Laan, G. P., de Haas, M. P., & Lutz, E. T. G. (1996). *Macromolecules*, *29*, 7362.
[9] Kepler, R.G., & Soos, Z.G. (1991). *Phys. Rev.*, *43*, 12530.
[10] Nespůrek, S., Sworakowski, J., Kadashchuk, A., & Toman, P. (2003). *J. Orgmet. Chem.*, *685*, 269.
[11] Němec, H., Kratochvılova, I., Kuěl, P., Šebera, J., Kochalska, A., Nožar, J., & Nešpúrek, S. (2011). *Phys. Chem. Chem. Phys.*, *13*, 2850.
[12] Toman, P., Nespůrek, S., Jang, J.W., & Lee, C.E. (2002). *Curr. Appl. Phys.*, *2*, 327.
[13] Chang, Jui-Fe., Sirringhaus, H., Giles, M., Heeney, M., & McCulloch, I. (2007). *Phys. Rev. B*, *76*, 205204 x.
[14] Kepler, R.G., Zeiger, J.M., & Kurzt, S.R. (1987). *Phys.Rev.*, *B*, *35*, 2818.
[15] Fujino, M. (1987). *Chem. Phys. Let.*, *136*, 451.
[16] (a) Gorban, I. S., Gumenyuk, A. F., & Ya. Degoda, W. (1993). *Optics and spectroscopy (SU)*, *75*, 47. (b) Gorban, I. S., Gumenyuk, A. F., & Kutovyi, S. J. (1995). *J. Phys. (Ukraine)*, *40*, 73. (c) Gumenyuk, A. F., Ochrimenko, O. B., & Kutovyi, S. J. (1997). *J. Phys. (Ukraine)*, *42*, 870. (d) Gumenyuk, A. F., Grebenovych, M., & Kutovyi, S. J. (2002). *Functional Materials*, *9*, 14. (e) Gumenyuk, A. F. & Kutovyi, S. J. (2003). *Central European J. Phys.*, *1*, 307. (f) Gumenyuk, A. F. & Kutovyi, S. J. (2005). *Ukr. J. Phys. (eng.)*, *50*, 1125. (g) Gumenjuk, A. F., Kutovyi, S. J., Pachshenko,

V., & Stanovyi, O. (2009). *Ukr. J. Phys.*, *54*, 999; or http://arxiv.org/abs/1003.5573 29 Mar 2010, 1003.5573v1 [physics.optics].
[17] Chunwachirasiri, W., West, R., & Winokur, M. J. *Macromolecules*, *33*, 9720.
[18] Miller, R. D. & Michl, J. (1989). *Chem. Rev.*, *89*, 1359.
[19] KariKari, E. K., Greso, A. J., Farmer, B. L., Miller, R. D., & Rabolt, J. F. (1993). *Macromolecules*, *26*, 3937.
[20] West, R. (2003). *J. Orgmet. Chem.*, *685*, 6.
[21] Patnaik, S.S. & Farmer, B.L. (1992). *Polymer*, *33*, 4443.
[22] Winokur, M.J. & West, R. (2003). *Macromolecules*, *36*, 7338.
[23] Ottoson, C.H. & Michl, J. (2000). *J.Phys. Chem.*, *104*, 3367.
[24] Ungar, G. (1993), *Polymer*, *34*, 2050.
[25] Leites, L. A., Bukalov, S. S., Yadritzeva, T. S., Mokhov, M. K., Antipova, B. A., Frunze, T. M., & Dement'ev, V. V. (1992). *Macromolecules*, *25*, 2991.
[26] Fogarty, H.A., Ottosson, C.-H., & Michl, J. (2000). *J. Molec. Struct/(Theochem)*, *506*, 243.
[27] Farmer, B. L., Rabolt, J. F., & Miller, R. D. (1987). *Macromolecules*, *20*, 1167.
[28] WELSH, W. J. (1993). *Adv. Pol. Techn.*, *12*, 379.
[29] Ostapenko, N. I., Zaika, V., Suto, S., & Watanabe, A. (2004). *Optics and Spectroscopy*, *96*, 520.
[30] Kyotani, H., Shimomura, M., Miyazaki, M., & Ueno, K. (1995). *Polymer*, *36*, 915.
[31] Bukalov, S. S., Leites, L. A., & West, R. (2001). *Macromolecules*, *34*, 6003.
[32] Bukalov, S. S., Teplitsky, M. V., Gordeev, Yu. Yu., Leites, L. A., & West, R. (2003). *Rus. Chem. Bul. Int. Edit.*, , 1066.
[33] Bukalov, S. S., Zubavichus, Y. V., Leites, L. A., Koe, J. R., & West, R. (2009). *Polymer*, *50*, 4845.
[34] Ostapenko, N., Kozlova, N., Suto, S., & Watanabe, A. (2006). *Low Temperature Physics*, *32*, 1035.
[35] Dementjev, A., Gulbinas, V., Ostapenko, L.Valkunas,N., Suto, S., & Watanabe, A. (2007). *J. Phys. Chem. C*, *111*, 4717.